Examination of a climate stabilization pathway via zero-emissions using Earth system models

2015 Environ. Res. Lett. 10 095005

(http://iopscience.iop.org/1748-9326/10/9/095005)

Environmental Research Letters

LETTER

Examination of a climate stabilization pathway via zero-emissions using Earth system models

Daisuke Nohara[1], J Tsutsui[1], S Watanabe[2], K Tachiiri[2], T Hajima[2], H Okajima[2] and T Matsuno[2]

[1] Central Research Institute of Electric Power Industry, Abiko, Japan
[2] Japan Agency for Marine-Earth Science and Technology, Yokohama, Japan

E-mail: nohara@criepi.denken.or.jp

Keywords: zero emissions, cumulative emissions, Earth system model, carbon cycle, climate stabilization

Supplementary material for this article is available online

OPEN ACCESS

RECEIVED
30 April 2015

REVISED
3 August 2015

ACCEPTED FOR PUBLICATION
7 August 2015

PUBLISHED
2 September 2015

Abstract

Long-term climate experiments up to the year 2300 have been conducted using two full-scale complex Earth system models (ESMs), CESM1(BGC) and MIROC-ESM, for a CO_2 emissions reduction pathway, termed Z650, where annual CO_2 emissions peak at 11 PgC in 2020, decline by 50% every 30 years, and reach zero in 2160. The results have been examined by focusing on the approximate linear relationship between the temperature increase and cumulative CO_2 emissions. Although the temperature increase is nearly proportional to the cumulative CO_2 emissions in both models, this relationship does not necessarily provide a robust basis for the restriction of CO_2 emissions because it is substantially modulated by non-CO_2 forcing. CO_2-induced warming, estimated from the atmospheric CO_2 concentrations in the models, indicates an approximate compensation of nonlinear changes between fast-mode responses to concentration changes at less than 10 years and slow-mode response at more than 100 years due to the thermal inertia of the ocean. In this estimate, CESM1 (BGC) closely approximates a linear trend of 1.7 °C per 1000 PgC, whereas MIROC-ESM shows a deviation toward higher temperatures after the emissions peak, from 1.8 °C to 2.4 °C per 1000 PgC over the range of 400–850 PgC cumulative emissions corresponding to years 2000–2050. The evolution of temperature under zero emissions, 2160–2300, shows a slight decrease of about 0.1 °C per century in CESM1(BGC), but remains almost constant in MIROC-ESM. The fast-mode response toward the equilibrium state decreases with a decrease in the airborne fraction owing to continued CO_2 uptake (carbon cycle inertia), whereas the slow-mode response results in more warming owing to continued heat uptake (thermal inertia). Several specific differences are noted between the two models regarding the degree of this compensation and in some key regional aspects associated with sustained warming and long-term climate risks. Overall, elevated temperatures continue for at least a few hundred years under zero emissions.

1. Introduction

Numerous studies have suggested that the globally averaged temperature response is approximately proportional to cumulative CO_2 emissions (e.g., Matthews and Caldeira 2008, Allen *et al* 2009, Matthews *et al* 2009, Solomon *et al* 2009). This means that the temperature increases with CO_2 emissions and that the elevated temperature would remain approximately constant even if emissions reach zero in the future. This proportional relationship essentially arises from the compensation of radiative forcing change and thermal inertia of the ocean (Matthews *et al* 2009), which involves several nonlinear effects such as the logarithmic nature of CO_2 forcing, changes in the airborne fraction of CO_2 resulting from carbon cycle processes and their interaction with climate, and long-term evolution of ocean heat uptake. Recent studies have explored these effects quantitatively by using analytical formulation and have discussed the reasoning behind the compensation (Goodwin *et al* 2015, MacDougall and Friedlingstein 2015). In the framework of cumulative CO_2 emissions, the role of non-CO_2 greenhouse gases has also been considered

regarding emission trajectories (Raupach 2013) and the persistent nature of warming (Solomon *et al* 2010, Frölicher and Joos 2010).

The proportional relationship, or persistent warming following the cessation of CO_2 emissions, has been well established by numerical experiments with Earth system models (ESMs) of intermediate complexity (e.g., Plattner *et al* 2008, Eby *et al* 2009, Zickfeld *et al* 2013, Herrington and Zickfeld 2014). Although full-scale complex ESMs essentially support these findings (Lowe *et al* 2009, Gillett *et al* 2011, Gillett *et al* 2013), exceptional behavior has been found in the long-term temperature response depending on the model and emissions pathway used in a particular experiment (Nohara *et al* 2013, Frölicher *et al* 2014). Despite the uncertainties, using complex ESMs is the only way to explore the spatial distribution of the temperature response and other relevant climate variables (e.g., Zickfeld *et al* 2012). Among others, Nohara *et al* (2013) reported that the behavior of the Atlantic meridional overturning circulation (AMOC) after the cessation of emissions depends on the emissions pathways even for the same total amount and that weakening of AMOC contributes little to changes in the global ocean carbon cycle.

These past studies are largely based on idealized emissions pathways resulting in a large signal-to-noise response to facilitate better analysis of the model behavior. In contrast, the present study focuses on the response of complex ESMs to more plausible emissions pathway in the context of climate change mitigation policies and socioeconomic feasibility. One such emissions pathway, Z650, has been proposed and discussed by Matsuno *et al* (2012a, 2012b). Z650 is designed on the basis of the 'zero-emissions stabilization' concept, which targets the reduction of CO_2 emissions to zero in the distant future, typically in the middle of the 22nd century. Under this framework, the atmospheric CO_2 concentration is reduced by natural removal processes and eventually reaches stable equilibrium. The amount of CO_2 emissions is 652 PgC during the 21st century, and the cumulative total from the middle of the 19th century, a common starting point for historical climate experiments, is 1101 PgC. The name 'Z650' implies reaching zero following approximately 650 PgC during the 21st century.

Z650 is intended to allow more emissions during the 21st century from a socioeconomic viewpoint compared with the rather stringent mitigation scenarios such as RCP2.6, the lowest forcing level among the four representative concentration pathways (RCPs) (Moss *et al* 2010). In fact, the CO_2 emissions of 650 PgC are between RCP2.6 and the second-lowest, RCP4.5. According to the scenario categories of the Intergovernmental Panel on Climate Change Working Group III (Clarke *et al* 2014), Z650 belongs to the 530–580 ppmCO_2eq category in case of a simple climate modeling exercise conducted by Matsuno *et al* (2012b), in which non-CO_2 forcing of 0.65 Wm^{-2} is assumed at the end of the 21st century and beyond. Moreover, Z650 is intended to avoid long-term serious climate risks, such as ice-sheet melting in Greenland, by a long-lasting decrease in the atmospheric CO_2 concentration under zero emissions and a subsequent decrease in the temperature by about 1 °C or less on a multiple century timescale. This concept, however, may not be compatible with the persistent nature of the temperature response. The present study investigates the details of climate system behavior in the Z650 pathway by using two different ESMs and discusses the implications for long-term climate stabilization in light of the zero-emissions stabilization concept.

2. Method

2.1. Models

The ESMs used in this study are the National Center for Atmospheric Research Community Earth System Model version 1 Biogeochemistry (CESM1(BGC)) (Hurrell *et al* 2013) and the ESM based on Model for Interdisciplinary Research on Climate (MIROC-ESM; Watanabe *et al* 2011). Both models are included in the fifth phase of the Coupled Model Intercomparison Project (CMIP5) (Taylor *et al* 2012) and are categorized as among the most comprehensive ESMs, incorporating full biogeochemical processes with no flux adjustments to represent the climate–carbon cycle in atmosphere–ocean general circulation.

CESM1(BGC) has a uniform horizontal resolution of 1.25 × 0.9° (zonal/meridional grid) with 26 vertical levels in the atmosphere and a horizontal resolution of 1.11° × 0.27–0.54° with 60 vertical levels in the ocean. The terrestrial carbon cycle is coupled to biogeophysical and hydrological processes, simulating photosynthesis, respiration, litter, and soil carbon and leaf phenology (Thornton *et al* 2007). The ocean carbon cycle component is based on the nutrient–phytoplankton–zooplankton–detritus approach represented by the biogeochemical element cycling model (Moore *et al* 2004).

MIROC-ESM has a horizontal resolution of T42, approximately 2.8°, with 80 vertical levels in the atmosphere and a horizontal resolution of 1.4° × 0.5–1.7° with 44 levels in the ocean. MIROC-ESM is coupled with the spatially explicit individual-based dynamic global vegetation model (SEIB-DGVM) for the terrestrial ecosystem (Sato *et al* 2007), which adopts a scheme that explicitly captures light competition among trees rather than using parameterized schemes. The ocean carbon cycle component in this model is also based on the nutrient–phytoplankton–zooplankton–detritus approach (Oschlies 2001).

Table 1 summarizes the primary features of climate change and the carbon cycle in CESM1(BGC) and MIROC-ESM. The values for equilibrium climate sensitivity (T_{ECS}), which is defined as the global

Table 1. Primary features of climate change and the carbon cycle.

	CESM1(BGC)	MIROC-ESM
Equilibrium climate sensitivity (°C)[a]	2.89	4.67
Adjusted radiative forcing ($2xCO_2$) (Wm^{-2})[a]	3.57	4.26
Carbon sensitivity (terrestrial)[b]	High	Moderate
Carbon sensitivity (ocean)[b]	Moderate	Moderate
Carbon-climate feedback[b]	Positive weak	Positive strong
Reference	Hurrell *et al* (2013)	Watanabe *et al* (2011)

[a] Estimated by Forster *et al* (2013).

[b] Based on a multi-model intercomparison by Arora *et al* (2013).

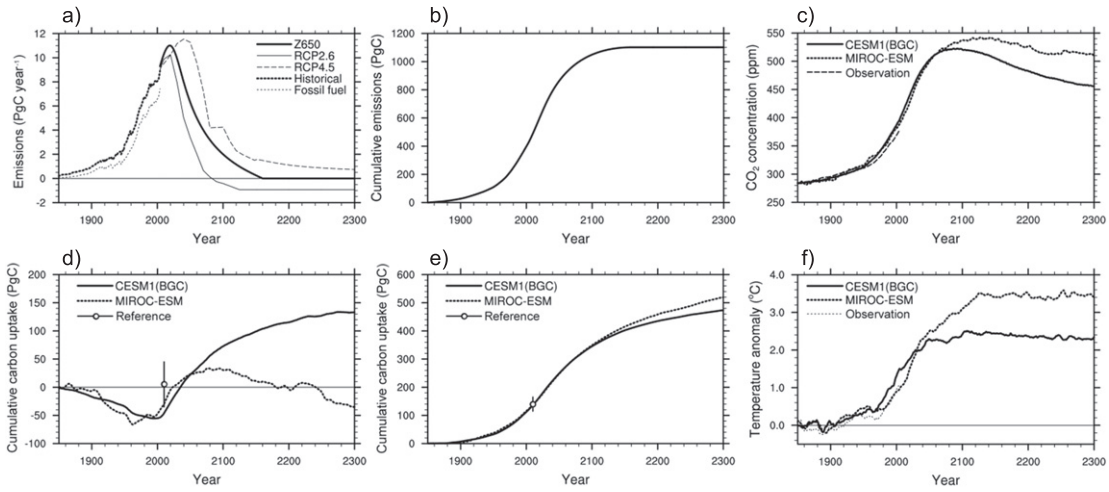

Figure 1. Time series of biogeochemical and physical climate variables: (a) CO_2 emission pathways, (b) cumulative CO_2 emissions, (c) atmospheric CO_2 concentration, (d) cumulative carbon uptake by land, (e) cumulative carbon uptake by ocean, and (f) globally averaged surface air temperature anomalies relative to the period 1850–1869. Panel (a) contains historical emissions from fossil fuels combustion and land use changes and two of representative concentration pathways. Panels (a), (c)–(f) contain reference data: (a), (c) Meinshausen *et al* (2011), (d) and (e) cumulative carbon uptake at present by the best estimate (open circle) and uncertainty (bar) (Ciais *et al* 2013), (f) HadCRUT4 (Morice *et al* 2012). The climate drift of the temperature anomalies has been removed. The carbon flux and temperature data are smoothed using a 9-year running mean.

equilibrium surface–air–temperature change in response to doubling of the atmospheric CO_2 concentration, are 2.89 °C and 4.67 °C in CESM1(BGC) and MIROC-ESM, respectively (Andrews *et al* 2012, Forster *et al* 2013). T_{ECS} for CESM1(BGC) (MIROC-ESM) is moderate (highest) in the CMIP5 model range, from 2.08 °C to 4.67 °C (Andrews *et al* 2012, Forster *et al* 2013). The carbon sensitivity and climate–carbon feedback were evaluated by Arora *et al* (2013). The carbon sensitivity is defined as the increase in atmospheric CO_2 in response to CO_2 emissions, as determined by the strength of natural carbon sinks (Matthews *et al* 2009). The climate–carbon feedback is defined as the reduction of terrestrial and oceanic CO_2 uptake caused by the increase in temperature. Among CMIP5 ESMs, the terrestrial model processes in CESM1(BGC) result in higher carbon sensitivity, which is explained mainly by a suppressed CO_2 fertilization effect due to nitrogen limitation (Bonan and Levis 2010). In contrast, MIROC-ESM has a moderate carbon sensitivity on land; that in the ocean is moderate for the both models. The behavior of the carbon–climate feedback differs considerably between CESM1 (BGC) and MIROC-ESM. In positive carbon–climate feedback, higher temperatures increase the flux of carbon from the land and ocean into the atmosphere, and the resulting higher atmospheric CO_2 concentration enhances warming. Although both models have positive feedback, its magnitude is weak in CESM1(BGC) but strong in MIROC-ESM. On the whole, CESM1 (BGC) and MIROC-ESM have a tendency to project a higher airborne fraction of cumulative emissions among CMIP5 ESMs (Arora *et al* 2013).

2.2. Experimental design

Figure 1(a) shows a time series of Z650 carbon emissions from the year 2005 following historical carbon emissions by fossil fuels and land use change; this series is compared with RCP 2.6 and RCP 4.5 from the year 2005 and their extension to 2300 (Meinshausen *et al* 2011). The Z650 pathway, located between RCP 2.6 and RCP 4.5, peaks in 2020 with 11 PgC and reaches zero in 2160. The amount of annual emissions declines during this period roughly at a rate of 50% every 30 years. Figure 1(b) shows a time series of the cumulative total of the historical and Z650 CO_2

Table 2. Linear trends of atmospheric CO_2 concentration and global mean surface temperature anomaly during the period 2160–2300.

	CESM1(BGC)	MIROC-ESM
CO_2 concentration (ppm yr^{-1})	−0.32	−0.16
Temperature (°C per century)	−0.083	0.004

emissions. The cumulative emissions reach 400 PgC in the year 2000 and 860 PgC in the year 2050.

We conducted historical and Z650 emission-driven experiments by using CESM1(BGC) and MIROC-ESM. These models prognostically compute global atmospheric CO_2 mole fractions, which represent an integration of physical, chemical, and biological processes with land use change, and their interactions and feedbacks with the climate system. The historical experiments, corresponding to experiment 5.2 or esmHistorical of CMIP5 (Taylor *et al* 2012), are forced by spatially distributed CO_2 emissions reconstructed from fossil fuel consumption estimates (Andres *et al* 2011) since 1850. The historical forcing also includes land use change and concentrations of non-CO_2 greenhouse gases such as methane, nitrous oxide, and halocarbons in addition to aerosols. At the end of the historical period, CO_2 forcing is altered to match Z650, which is implemented as the reconstructed fossil emissions in 2005 scaled by the global total emissions along the Z650 pathway. Land use is not changed after 2005, although some delayed emissions from land use changes in the historical period are accounted for. Other non-CO_2 greenhouse gases and aerosols follow RCP 2.6 (van Vuuren *et al* 2011) for the period 2005–2100 and are kept constant after 2100.

3. Results and discussion

3.1. Biogeochemical and climate changes

The atmospheric CO_2 concentrations calculated by the two ESMs both show a peak-and-decline evolution in response to the Z650 CO_2 emissions, as illustrated in figure 1(c). The peak level and time in CESM1 (BGC) and MIROC-ESM are 520 ppm in the year 2080 and 540 ppm in the year 2120, respectively. This difference simply reflects the different amounts of carbon uptake by natural processes because land use is unchanged by the experiment design. At the end of the experiment period, at year 2300, the concentrations and their decreasing trends since the emissions level has reached zero, at year 2160, are about 455 ppm and 510 ppm, and −0.32 ppm yr^{-1} and −0.16 ppm yr^{-1}, respectively, in CESM1(BGC) and MIROC-ESM (table 2). It should be noted that both models have a positive bias; the concentration at the end of the historical period is 20 ppm and 12 ppm, respectively, above the observed level compiled by Meinshausen *et al* (2011).

The amounts of accumulated land and ocean carbon are shown in figures 1(d) and (e) with observed estimates in the year 2010 (Ciais *et al* 2013) for reference. At this reference time for both models, land carbon is underestimated whereas ocean carbon is comparable to the observed estimates. In response to the Z650 emissions under fixed land use, land carbon increases toward an apparent equilibrium level in CESM1(BGC), whereas it peaks by the end of the 21st century, then declines to negative values in MIROC-ESM owing to its strong carbon–climate feedback. The cumulative carbon uptake by the year 2300 is 132 PgC in CESM1(BGC) and −35 PgC in MIROC-ESM.

Carbon accumulation in the ocean continues throughout the experiment period in both ESMs. However, a decline in the accumulation growth rate noted in both models is more discernible in CESM1 (BGC). This difference is understood to originate from an interaction of the land and ocean uptake processes such that a larger land uptake in CESM1(BGC) makes the atmospheric concentration lower, which suppresses the ocean uptake owing to a smaller difference of CO_2 pressure between the atmosphere and ocean. The cumulative carbon uptake by the year 2300 is 475 PgC in CESM1(BGC) and 520 PgC in MIROC-ESM.

Figure 1(f) displays the temporal evolution of the globally averaged surface air temperature anomalies relative to the years 1850–1869. Climate drift components, obtained from a linear trend during the period 1850−2300 in the preindustrial control of −0.008 °C per century in CESM1(BGC) and 0.102 °C per century in MIROC-ESM, were removed. In the year 2005, CESM1(BGC) is about 0.4 °C higher than observation by HadCRUT4 (Morice *et al* 2012), although MIROC-ESM is comparable to observation. After a rapid increase until about 2050, both models show decelerated warming. In CESM1(BGC), the temperature anomaly peaks at about 2.5 °C around the year 2100, then slightly decreases at a rate of about 0.1 °C per century (table 2). The temperature anomaly in MIROC-ESM peaks at about 3.5 °C around the year 2130 and subsequently remains almost constant. Overall, both ESMs show elevated temperature anomalies that continue for at least a few hundred years in response to the Z650 emissions pathway. This long-term tendency is essentially consistent with the energy budget of the model, which includes radiative forcing and ocean heat uptake (supplement 1). In addition, this trend is explained by the thermal inertia of the ocean and the logarithmic nature of CO_2 forcing, which results in a small decrease in forcing relative to the concentration decrease (Solomon *et al* 2010).

3.2. Proportionality of the transient climate response to cumulative emissions

Figure 2(a) shows globally averaged surface air temperature anomalies as a function of cumulative carbon

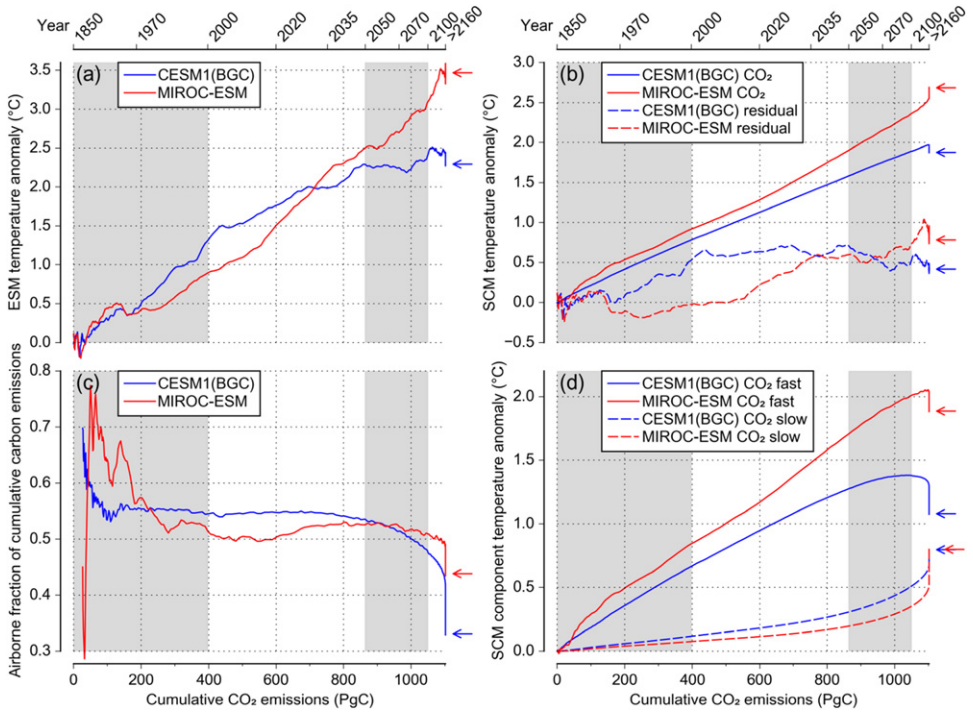

Figure 2. (a) Globally averaged surface air temperature anomalies relative to 1850–1869 as a function of cumulative total global CO_2 emissions. (b) As for (a), but estimates of CO_2-induced temperature anomalies and residuals are shown. Fast and slow components of these CO_2-induced temperature anomalies are shown in (d). (c) As for (a), but airborne fractions of cumulative emissions are shown. Emissions in the historical period include those from land use changes in CESM1(BGC), which are also applied for MIROC-ESM in these diagrams because land use emissions are not isolated in MIROC-ESM. Arrows in the right margins indicate averages over the last decade, and the trajectory along the right edge of each diagram indicates a change during the zero-emissions period (2160–2300). Note that the end point of the trajectory is not necessarily the same as the last time. Some reference time points are shown in the upper horizontal axis, and the periods of 1850–2000 and 2050–2100 are shaded.

emissions. Although both ESMs show a somewhat proportional relationship between temperature change and cumulative emissions, noticeable differences are apparent in the trajectories on the temperature–cumulative emissions diagram. Overall, the trajectory is curved downward (upward) in CESM1 (BGC) (MIROC-ESM). Figure 2(b) shows the components of CO_2-induced change and residual one on the same diagram as that shown in figure 2(a), which were calculated by using a simple climate model (SCM) with an assumption of linear forcing additivity (supplement 2). The component trajectories for the CO_2-induced change in both ESMs are approximately consistent with those from the 1% per year CO_2 increase experiments of CMIP5 (figure 1(a) in Gillett *et al* 2013). The CO_2-induced temperature anomaly in response to 1000 PgC emissions, termed transient climate response to cumulative carbon emissions (TCRE), is 1.8 °C in CESM1(BGC) and 2.2 °C in MIROC-ESM, ranked as middle and high, respectively, across the CMIP5 models.

A comparison of the component and the total trajectories reveals that the larger total warming in CESM1(BGC) despite its lower climate sensitivity from 200 PgC to 700 PgC in 1970–2030 period is due mainly to different implementation of non-CO_2 forcing. Other factors relevant to this anomalous response include different response characteristics (supplement 2) and decadal climate variability. Although the two ESMs deal with common forcing agents, the cooling effect due to aerosol–cloud interaction is not implemented in CESM1(BGC) (table 12.1 in Collins *et al* 2013). The aerosol–cloud interaction is quantified as $-0.45\ \mathrm{Wm}^{-2}$ with 90% uncertainty of $-1.2\ \mathrm{Wm}^{-2}$ to $0.0\ \mathrm{Wm}^{-2}$ in terms of effective radiative forcing from 1750 to 2011 (Myhre *et al* 2013). Apart from the uncertainty of the forcing magnitude and its efficacy on the temperature response, the absence of this cooling effect is large enough to create a warm bias in the early 21st century in CESM1(BGC) (Hurrell *et al* 2013). In the later period, when non-CO_2 forcing does not much affect differences between the two models, the residual component for MIROC-ESM is comparable to or higher than that for CESM1(BGC), where decadal fluctuations imply the models' internal variability. Trajectories for the CO_2-induced temperature indicate an approximately linear relationship in CESM1(BGC), while MIROC-ESM shows a deviation toward higher temperatures after the emissions peak. Over the range of 400–850 PgC corresponding to years 2000–2050, the warming rate per 1000 PgC is 1.7 °C in CESM1(BGC), while changes from 1.8 °C to 2.4 °C at about 600 PgC in MIROC-ESM.

Compared with idealized emissions pathways in existing studies, Z650 is a plausible mitigation pathway in which the amount of annual CO_2 emissions peaks in the year 2020 and reaches zero after 140 years. Moreover, the atmospheric CO_2 concentration experiences periods of rapid growth, decelerating growth, and decline. Here, we decompose the CO_2-induced temperature response into fast and slow components with distinct timescale separation to facilitate the analysis of the temperature and cumulative emissions relationship in these different phases. The temperature response in the SCM is formulated as the sum of three exponentials. We define the fast and slow mode responses as the sum of two exponentials with a smaller time constant of less than 10 years and that with a longer time constant of more than 100 years, respectively. Normalized amplitudes of the fast and slow mode responses are about 0.6 and 0.4, respectively, for both ESMs (table S1). Because the fast component roughly corresponds to changes in radiative forcing, its relationship to cumulative CO_2 emissions is close to a logarithmic function, depending on the extent to which the airborne fraction is stable. In addition, the fast-mode response reflects the continued CO_2 uptake, or carbon cycle inertia, predominantly by the ocean, which alters the airborne fraction. The slow component represents delayed response due to thermal inertia. Because the emissions reduction period of 140 years is comparable to the timescale of the slow component, this response essentially increases nonlinearly in terms of the cumulative emissions.

The decomposed temperature response and the airborne fraction as a function of cumulative emissions, are shown in figures 2(c) and (d). The first half of the 21st century is characterized by a peak-and-decline annual emissions change, with a peak at 11 PgC in 2020 and a decrease to 8 PgC in 2040). In this period, the atmospheric CO_2 concentration increases, although the rate of increase gradually becomes smaller. In addition, the carbon cycle in CESM1(BGC) behaves such that the airborne fraction remains approximately constant and then declines, whereas that in MIROC-ESM results in a temporary increase at about 600 PgC, corresponding to the peak year of 2020. The fast temperature response should increase logarithmically for a constant airborne fraction. This logarithmic trend, however, does not deviate significantly from the linear trend for additional emissions of a few hundred petagrams of carbon during this period. In the case of MIROC-ESM, the airborne fraction increase overcomes the logarithmic forcing effect, and results in an increased gradient for the fast-mode response trajectory as well as the total one discussed above.

In the second half of the 21st century, characterized by a continued annual emissions reduction at a constant time rate of 50% every 30 years to 2 PgC in 2100, long-term changes associated with carbon cycle inertia and thermal inertia appear more evident. The airborne fraction gradually decreases in MIROC-ESM, However, this decreasing rate is considerably smaller than that in CESM1(BGC), which causes the divergence in the fast-mode responses between the two ESMs. The slow temperature response increases with cumulative emissions at a greater rate than in the earlier period. This nonlinear increase compensates for the logarithmic fast response, resulting in the approximate linear relationship between temperature and cumulative emissions in this period for both ESMs. In the case of CESM1(BGC), this compensation is already discernible in the first half of the 21st century. The slow-mode response is greater in CESM1(BGC) because of its smaller time constant (table S1), which has a greater effect than the difference in climate sensitivity for a transient state.

Beyond the 21st century, characterized by the achievement of zero emissions in year 2160 and evolution toward a quasi-equilibrium state on a millennial timescale, the thermal inertia increases the temperature in the slow-mode response whereas the carbon cycle inertia compensates this increase through the fast-mode response. Regarding the magnitude of this compensation under zero emissions in 2160–2300, noticeable differences are apparent between the two models, as indicated by trajectories along the right edge of the diagrams in figure 2. Although the airborne fraction decreases in both ESMs, this decrease and its effect on the fast-mode response are smaller in MIROC-ESM. Moreover, the increase in the slow-mode response is greater in MIROC-ESM, which is explained by its higher climate sensitivity and longer time constant. These differences result in different developments of the CO_2-induced warming, shown as a subtle decrease (increase) in CESM1(BGC) (MIROC-ESM) of 0.07 °C (0.1 °C) per century.

These changes still represent a transient stage from the viewpoint of climate stabilization on a millennial timescale. It is expected that long-term processes will continue beyond 2300 and that the temperature response trends may continue or move in a different direction.

3.3. Some remarks on regional changes

The Z650 concept regarding long-term climate change mitigation considers that a severe climate risk due to melting of the Greenland ice sheet is avoidable as long as sustained high temperatures are limited within a few hundred years. Here, we focus on several regional aspects associated with sustained changes and those in the Arctic region.

Figure 3 illustrates the spatial distribution of temperature change during the zero emissions period of 2160 to 2300. Both ESMs generally project a decreasing temperature trend in the Northern Hemisphere because of the reduction of radiative forcing. In contrast, the Southern Hemisphere high-latitude region surrounding the Antarctic experiences continuous

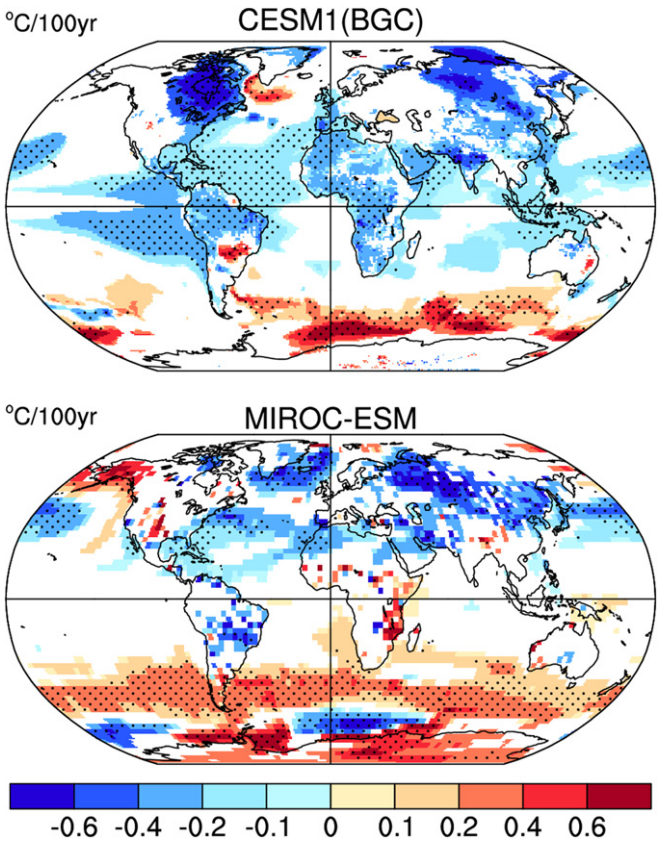

Figure 3. Distribution of regression coefficients for surface air temperature during the zero emission period in (upper) CESM1(BGC) and (lower) MIROC-ESM. Stippling indicates regions where the level of confidence is greater than 99%. White areas indicate regions where the level of confidence is less than 90%. The climate drift has been removed at each grid point.

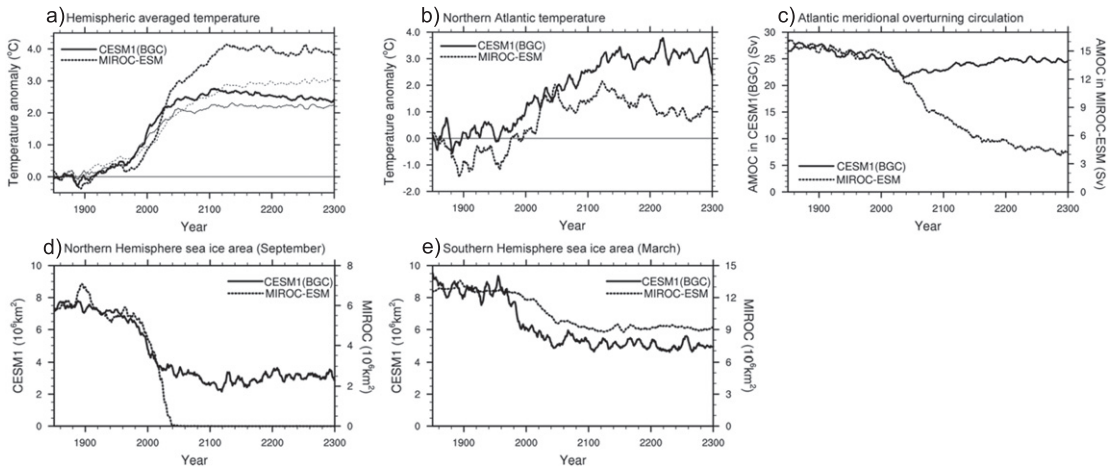

Figure 4. Time series of physical climate variables smoothed using a a 9-year running mean: (a) surface air temperature anomaly in the Northern Hemisphere (bold) and Southern Hemisphere (thin) relative to the years 1850–1869, (b) surface air temperature anomaly in the North Atlantic region (55 °N–70 °N, 10 °W–60 °W) relative to the years 1850–1869, (c) Atlantic meridional overturning circulation (AMOC) in Sverdrup (1 Sv $= 10^6$ m^3 s^{-1}), (d) Northern Hemisphere sea ice area in September, and (e) Southern Hemisphere sea ice area in March.

warming caused by thermal inertia of the ocean. Although these spatial distributions are generally consistent with the previous zero emission study by Gillett *et al* (2011), several regional differences exist between the two models, such as that shown in the Southern Ocean. These differences might affect the global temperature response, considering that other modeling studies focusing on the role of the ocean circulation in the heat uptake (Winton *et al* 2013, Frölicher *et al* 2015).

Figure 4 shows the temporal evolutions of selected regional variables. Although the hemisphere-scale

surface air temperatures show a similar long-term tendency between the two models (figure 4(a)), the temperatures over some regions, typically those in the northern Atlantic area surrounding Greenland (figure 4(b)), show opposing temperature trends (figure 3). After the year 2100, the temperature slightly decreases in MIROC-ESM but remains almost constant in CESM1(BGC). In addition, the temperature in MIROC-ESM is lower than in CESM1(BGC) despite the higher equilibrium climate sensitivity of MIROC-ESM. In general, it is expected that the decreasing temperature trend in the Northern Hemisphere reduces the risk of Greenland ice sheet melting, even though elevated temperatures continue globally for a few hundred years or more. However, such melting might be affected by several local aspects that are subject to model dependency and uncertainties.

The temperature in the northern Atlantic region is sensitive to AMOC, which is quantified by the maximum stream function of the meridional overturning transport for the Atlantic basin between 30 °N and 50 °N below the depth of 500 m (figure 4(c)). In CESM1(BGC) the strength of AMOC weakens temporarily and recovers to a preindustrial level. However, that in MIROC-ESM gradually weakens throughout the experiment period and reaches 4 Sv at the end, which corresponds to one-fourth of the preindustrial AMOC level. This different response may be related to the AMOC stability of models: MIROC-ESM has a characteristic bistable regime, whereas CESM1(BGC) has a monostable regime (Weaver *et al* 2012). The relatively lower temperatures surrounding Greenland in MIROC-ESM are explained by decreased poleward heat transport associated with the weakened AMOC. This finding implies that internal processes, rather than external CO_2 forcing, are crucial for temperature changes in this particular region.

Arctic sea ice in September disappears completely in MIROC-ESM by the year 2050. In CESM1(BGC), however, it reaches a minimum of about 3×10^6 km^2, or about 40% of the preindustrial level (figure 4(d)). Although the Arctic sea ice area in CESM1(BGC) slightly recovers after the year 2100, MIROC-ESM projects no sign of recovery. In either case, however, changes in the Arctic sea ice do not significantly affect the temperature trend in the Arctic region (figure 3). The Antarctic sea ice area in March in CESM1(BGC) and MIROC-ESM relatively reaches minimums of about 70% and 60% of the preindustrial level (figure 4(e)) at the end of the 21st century and later remains approximately constant in both models.

4. Conclusion

In this study, we conducted emission-driven experiments by using CESM1(BGC) and MIROC-ESM for the Z650 pathway, which is an illustrative long-term pathway of plausible CO_2 emissions reduction. In addition, we discussed global changes in the climate and carbon cycle in light of the approximately linear relationship between the temperature increase and cumulative CO_2 emissions. The Z650 annual CO_2 emissions peak at 11 PgC in 2020, allowing more emissions in the early part of the 21st century compared with the stringent mitigation scenarios such as RCP2.6 and assuming long-term climate change mitigation by natural CO_2 removal processes under zero emissions. Therefore, the key points are the transient temperature increase during the 21st century and the subsequent long-term temperature change under zero emissions. Because the Z650 concept for long-term climate mitigation considers the risk of Greenland's ice sheet melting, several regional aspects were also examined.

Although the transient temperature increase is nearly proportional to cumulative CO_2 emissions, this linear relationship is not necessarily a good indicator for an early part of the 21st century because it is modulated considerably by non-CO_2 forcing. Model biases during the historical period also affect near-future projections. CO_2-induced warming, estimated from the atmospheric CO_2 concentration by using a SCM, indicates a clearer linear relationship between temperature and cumulative CO_2 emissions. This linearity arises from the compensating effects of the fast (slow) mode for the temperature response with modulations by the airborne fraction, as indicated respectively by the logarithmic function (nonlinear upward-increase) shape. These components depend on characteristics of models such as climate and carbon sensitivity, climate–carbon cycle feedback, and timescales of the temperature response, as well as on emission pathways. In the case of Z650, CESM1(BGC) closely approximates a linear trend, whereas MIROC-ESM shows a deviation toward higher temperatures after the annual emissions peak due to an increase in the airborne fraction.

Regarding the long-term temperature change under zero emissions, the evolution of temperature until 2300 shows a slight decrease of about 0.1 °C per century in CESM1(BGC) compared with an almost constant value in MIROC-ESM. These changes are also affected by changes in non-CO_2 forcing during the 21st century. Analysis of the simple model for CO_2-induced warming indicates that the fast-mode temperature decreases in response to a decline in the airborne fraction due to carbon cycle inertia. This fast-mode decrease is largely compensated by the slow-mode increase due to thermal inertia. The magnitude of the relationship between the slow and fast modes is different between the two ESMs, resulting in different developments in the CO_2-induced warming, marked by a subtle decrease (increase) in CESM1(BGC) (MIROC-ESM) of 0.07 °C (0.1 °C) per century.

Overall, elevated temperatures continue for at least a few hundred years under zero emissions. The increasing trend in MIROC-ESM may be considered a

conservative estimate in the context of climate mitigation policy because the model's characteristics tend to produce higher airborne fractions and temperatures among the current ESMs. Nevertheless, both models project a decreasing temperature trend in the Northern Hemisphere, which reduces the risk of Greenland ice sheet melting from a long-term perspective. In the vicinity of Greenland, several differences exist between the two models associated with AMOC and the Arctic sea ice, which should be examined for both near-term and long-term climate risks. However, these aspects do not significantly affect global temperature. Because the Z650 is a plausible emissions pathway with a moderate level of cumulative emissions, these conclusions may differ from the findings of other idealized experiments forced by a much larger emissions level and its abrupt change.

Acknowledgments

We are grateful for discussions with and comments from A Oka at university of Tokyo, F O Bryan at the National Center for Atmospheric Research (NCAR), M Kawamiya at the Japan Agency for Marine-Earth Science and Technology, and M Ohba, Y Yoshida, and N Nakashiki at the Central Research Institute of Electric Power Industry (CRIEPI). CESM1(BGC) experiments were supported by joint collaborative research between CRIEPI and NCAR. This work was supported by the KAKUSHIN and SOUSEI Program of the Ministry of Education, Culture, Sports, Science, and Technology in Japan.

References

Allen M R *et al* 2009 Warming caused by cumulative carbon emissions towards the trillionth tone *Nature* **458** 1163–6

Andres R J, Gregg J S, Losey L, Marland G and Boden T A 2011 Monthly, global emissions of carbon dioxide from fossil fuel consumption *Tellus* B **63** 309–27

Andrew T, Gregory J M, Webb M J and Taylor K E 2012 Forcing, feedbacks and climate sensitivity in CMIP5 coupled atmosphere-ocean climate models *Geophys. Res. Lett.* **39** L09712

Arora V K *et al* 2013 Carbon–concentration and carbon–climate feedbacks in CMIP5 Earth system models *J. Clim.* **26** 5289–314

Bonan G B and Levis S 2010 Quantifying carbon-nitrogen feedbacks in the community land model (CLM4) *Geophys. Res. Lett.* **37** L07401

Ciais P *et al* 2013 Carbon and other biogeochemical cycles *Climate Change 2013: The Physical Science Basis. Contribution of Working Group I to the Fifth Assessment Report of the Intergovernmental Panel on Climate Change* ed T F Stocker, D Qin, G-K Plattner, M Tignor, S K Allen, J Boschung, A Nauels, Y Xia, V Bex and P M Midgley (Cambridge: Cambridge University Press)

Clarke *et al* 2014 Assessing transformation pathways *Climate Change 2014: Mitigation of Climate Change. Contribution of Working Group III to the Fifth Assessment Report of the Intergovernmental Panel on Climate Change* ed O Edenhofer *et al* (Cambridge: Cambridge University Press)

Collins M *et al* 2013 Long-term climate change: projections, commitments and irreversibility *Climate Change 2013: The Physical Science Basis. Contribution of Working Group I to the Fifth Assessment Report of the Intergovernmental Panel on Climate Change* ed T F Stocker, D Qin, G-K Plattner, M Tignor, S K Allen, J Boschung, A Nauels, Y Xia, V Bex and P M Midgley (Cambridge: Cambridge University Press)

Eby M, Zickfeld K, Montenegro A, Archer D, Meissner K J and Weaver A J 2009 Lifetime of anthropogenic climate change: millennial time scales of potential CO_2 and temperature perturbations *J. Clim.* **22** 2501–11

Forster P M *et al* 2013 Evaluating adjusted forcing and model spread for historical and future scenarios in the CMIP5 generation of climate models *J. Geophys. Res. Atmos.* **118** 1139–50

Frölicher T L and Joos F 2010 Reversible and irreversible impacts of greenhouse gas emissions in multi-century projections with the NCAR global coupled carbon cycle-climate model *Clim. Dyn.* **35** 1439–59

Frölicher T L, Winton M and Sarmiento J L 2014 Continued global warming after CO_2 emissions stoppage *Nat. Clim. Change* **4** 40–4

Frölicher T L *et al* 2015 Dominance of the Southern Ocean in anthropogenic carbon and heat uptake in CMIP5 models *J. Clim.* **28** 862–86

Gillett N P, Arora V K, Zickfeld K, Marshall S J and Merryfield W J 2011 Ongoing climate change following a complete cessation of carbon dioxide emissions *Nat. Geosci.* **4** 83–7

Gillett N P, Arora V K, Matthews D and Allen M R 2013 Constraining the ratio of global warming to cumulative CO_2 emissions using CMIP5 simulations *J. Clim.* **26** 6844–58

Goodwin P, Williams R G and Ridgwell A 2015 Sensitivity of climate to cumulative carbon emissions due to compensation of ocean heat and carbon uptake *Nat. Geosci.* **8** 29–34

Herrington T and Zickfeld K 2014 Path independence of climate and carbon cycle response over a broad range of cumulative carbon emissions *Earth Syst. Dyn.* **5** 409–22

Hurrell J W *et al* 2013 The community Earth system model: a framework for collaborative research *Bull. Am. Meteorol. Soc.* **94** 1339–60

Lowe J A *et al* 2009 How difficult is it to recover from dangerous levels of global warming? *Environ. Res. Lett.* **4** 014012

MacDougall A H and Friedlingstein P 2015 The origin limits of the near proportionality between climate warming and cumulative CO_2 emissions *J. Clim.* **28** 4217–30

Matsuno T, Maruyama K and Tsutsui J 2012a Stabilization of atmospheric carbon dioxide via zero emissions—an alternative way to a stable global environment: I. Examination of the traditional stabilization concept *Proc. Japan Acad.* B **88** 368–84

Matsuno T, Maruyama K and Tsutsui J 2012b Stabilization of atmospheric carbon dioxide via zero emissions—an alternative way to a stable global environment: II. A practical zero-emissions scenario *Proc. Japan Acad.* B **88** 385–95

Matthews H D and Caldeira K 2008 Stabilizing climate requires near-zero emissions *Geophys. Res. Lett.* **35** L04705

Matthew H D, Gillett N P, Stott P A and Zickfeld K 2009 The proportionality of global warming to cumulative carbon emissions *Nature* **459** 829–32

Meinshausen M *et al* 2011 The RCP greenhouse gas concentrations and their extensions from 1765 to 2300 *Clim. Change* **109** 213–41

Moore J K, Doney S D and Lindsay K 2004 Upper ocean ecosystem dynamics and iron cycling in a global three-dimensional model *Glob. Biogeochem. Cycles* **18** 1–21

Morice C P, Kennedy J J, Rayner N A and Jones P D 2012 Quantifying uncertainties in global and regional temperature change using an ensemble of observational estimates: the HadCRUT4 data set *J. Geophys. Res.* **117** D08101

Moss R H *et al* 2010 The next generation of scenarios for climate change research and assessment *Nature* **463** 747–56

Myhre G *et al* 2013 Anthropogenic and natural radiative forcing *Climate Change 2013: The Physical Science Basis. Contribution of Working Group I to the Fifth Assessment Report of the Intergovernmental Panel on Climate Change* ed T F Stocker,

D Qin, G-K Plattner, M Tignor, S K Allen, J Boschung, A Nauels, Y Xia, V Bex and P M Midgley (Cambridge: Cambridge University Press)

Nohara D, Yoshida Y, Misumi K and Ohba M 2013 Dependency of climate change and carbon cycle on CO_2 emission pathways *Environ. Res. Lett.* **8** 014047

Oschlies A 2001 Model-derived estimates of new production: new results point towards lower values *Deep-Sea Res.* II **48** 2173–97

Plattner G K *et al* 2008 Long-term climate commitments projected with climate-carbon cycle model *J. Clim.* **21** 2721–51

Raupach M R 2013 The exponential eigenmodes of the carbon-climate system, and their implications for ratios of responses to forcings *Earth Syst. Dyn.* **4** 31–49

Sato H, Itoh A and Kohyama T 2007 SEIB-DGVM: a new dynamic global vegetation model using a spatially explicit individual-based approach *Ecol. Modelling* **200** 279–307

Solomon S *et al* 2010 Persistence of climate changes due to a range of greenhouse gases *Proc. Natl Acad. Sci. USA* **107** 18354–9

Solomon S, Plattner G-K, Knutti R and Friedlingstein P 2009 Irreversible climate change due to carbon dioxide emissions *Proc. Natl Acad. Sci. USA* **106** 1704–9

Taylor K E, Stouffer R J and Meehl G A 2012 An overview of CMIP5 and the experiment design *Bull. Am. Meteorol. Soc.* **93** 485–98

Thornton P E *et al* 2007 Influence of carbon-nitrogen cycle coupling on land model response to CO_2 fertilization and climate variability *Glob. Biogeochem. Cycles* **21** GB4018

van Vuuren D P *et al* 2011 RCP2.6: exploring the possibility to keep global mean temperature increase below 2 °C *Clim. Change* **109** 95–116

Watanabe S *et al* 2011 MIROC-ESM 2010: model description and basic results of CMIP5-20c3m experiments *Geosci. Model Dev.* **4** 845–72

Weaver *et al* 2012 Stability of the Atlantic meridional overturning circulation: a model intercomparison *Geophys. Res. Lett.* **39** L20709

Winton M, Griffies S M, Samuels B L, Sarmiento J L and Frölicher T L 2013 Connecting change ocean circulation with changing climate *J. Clim.* **26** 2268–78

Zickfeld K *et al* 2013 Long-term climate change commitment and reversibility: an EMIC intercomparison *J. Clim.* **26** 5782–809

Zickfeld K, Arora V K and Gillett N P 2012 Is the climate response to CO_2 emissions path dependent? *Geophys. Res. Lett.* **39** L05703